



ELSEVIER

Thermochimica Acta 280/281 (1996) 401–415

thermochimica
acta

Viscosity and relaxation of glasses below the glass transition temperature¹

Manabu Koide*, Ryuji Sato, Takayuki Komatsu, Kazumasa Matusita

*Department of Chemistry, Nagaoka University of Technology, 1603-1 Kamitomioka cho,
Nagaoka, Niigata-ken 940-21, Japan*

Abstract

The fiber bending method has been used for the measurement of the viscosity of glasses below the glass transition temperature. It was found that the viscosities of as-drawn and pre-annealed glass fibers below the glass transition temperature increase with increasing pre-annealing temperature and time. It was also found that the viscosity approaches the extrapolated line from the Fulcher curve fitted at temperatures above the glass transition temperature. On the other hand, by analyzing the relaxation mechanism, it was found that the stretching parameter decreases with decreasing temperature, suggesting wider distribution of relaxation time at lower temperature. By extrapolation it was found that the stretching parameter is about 0.6 near the glass transition temperature. This means that at the glass transition temperature the relaxation mechanism consists of more than one mode.

Keywords: Annealed glass; DTA; Glass transition temperature; Glass viscosity; Relaxation mechanism; Relaxation in glasses; Residual stress; Stretching parameter

1. Introduction

The viscosity is one of the most important properties of a glass and its temperature-dependence and relaxation mechanism above the glass transition temperature have been studied by many researchers [1–9]. It is also well known that glass is rigid and brittle below its glass transition temperature. However, it was reported that glasses can be deformed by an external pressure or an electric field even below the glass transition temperature [10–13]. It is important to measure the viscosity below the glass transition

* Corresponding author.

¹ Dedicated to Professor Hiroshi Suga.

temperature for investigation of glass relaxation processes. It is well known [12–14] that below glass transition temperature, the viscosity changes remarkably with time, in a manner dependent on the relaxation mechanism. It is, therefore, expected that this relaxation mechanism can be revealed by analyzing the viscosity change with time, and its temperature dependence.

In our previous report, the deformations of fluoride and oxide glasses were measured below the glass transition temperatures using the fiber-bending method [14, 15]. In the fiber-bending method, the glass fiber is bent and heat-treated at constant temperatures below the glass transition temperature for various times; after the load is removed the remaining curvature radius is measured. The stress and the strain are calculated from the remaining curvature radius. This new method makes it possible to measure high viscosities in the range 10^{13} – 10^{16} Pa s [14,15].

In the present study, using this fiber-bending method, viscosity and relaxation below the glass transition temperature are investigated. Furthermore, the relationship between the structure of a glass at any temperature below the glass transition temperature and the relaxation mechanism was analyzed.

2. Theory and analytical procedures of deformation

2.1. Viscosity measurement

The principle and the procedures of the fiber-bending method were reported previously [14,15], and so are described here only briefly. The schematic diagram of the measurement procedure is given in Fig. 1. Glass fibers were wound on a cylinder and kept at various temperatures far below the glass transition range for different periods of time; they were then released and the bending radii of the deformed fibers were measured. Fig. 2 shows the stress distribution in a fiber bent by a moment M . The biggest stretch deformation of a fiber is at the outside surface of the fiber and it is known that the strain, ε , can be represented by the following equation [14,15];

$$\varepsilon(r) = \frac{r}{R_0} \quad (1)$$

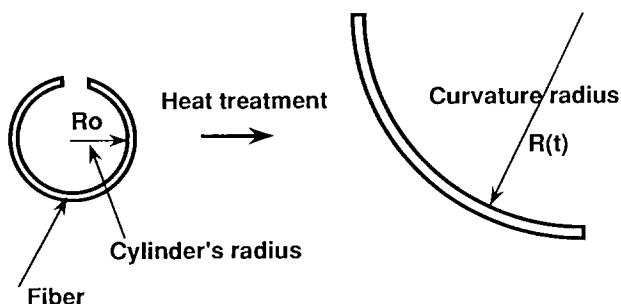


Fig. 1. Schematic diagram of measurement procedure.

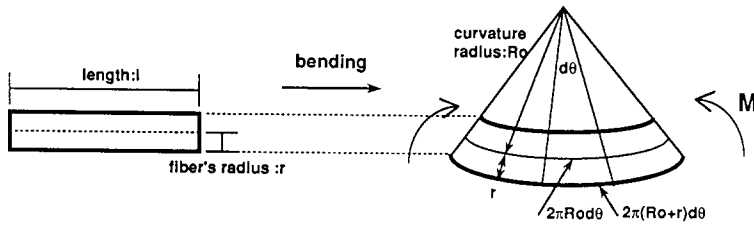


Fig. 2. The method of strain measurement of deformed fiber.

where r is the distance from the center line of the fiber to the outside surface and R_0 is the radius of curvature of the bending fiber. To estimate the bending stress, it is assumed that the elastic deformation obeys Hooke's Law ($\sigma = E\varepsilon$) and the elastic coefficient of the glass fiber is constant over the working temperature range. Consequently, the bending stress is expressed by

$$\sigma(r) = E \left(\frac{r}{R_0} \right) \tag{2}$$

where $\sigma(r)$ is the bending stress resulting from the application of a moment M , and E is Young's modulus. After the release of the applied stress, the fiber will not recover its initial form and partial deformation remains. This deformation is attributed to stress relaxation. Under constant strain, the stress decreases from the initial value, $\sigma(r, 0)$, to $\sigma(r, t)$ at time t .

$$\sigma(r, t) = \sigma(r, 0) - \sigma_{re}(r, t) \tag{3}$$

where $\sigma_{re}(t)$ is the relaxed stress until time t . The relaxed stress is expressed as follows,

$$\sigma_{re}(r, t) = E \cdot \varepsilon_{re}(r, t) = E \left(\frac{r}{R(t)} \right) \tag{4}$$

where $\varepsilon_{re}(r, t)$ is the residual strain and $R(t)$ is the radius of the deformed fibers after annealing for time t and release from the cylinder ($R(\infty) = R_0$). The viscosity, η , is expressed by the equation

$$\eta(t) = \frac{\sigma(r, t)}{3(d\varepsilon_{re}(r, t)/dt)} \tag{5}$$

where $d\varepsilon_{re}/dt$ is the rate of strain that can be evaluated from the plot of strain, ε_{re} , versus time. Using Eqs. (3) and (4), Eq. (5) can be rewritten as follows.

$$\eta(t) = E \frac{\frac{1}{R_0} - \frac{1}{R(t)}}{3d(1/R(t))/dt} \tag{6}$$

2.2. Relaxation mechanism

As mentioned above, it is considered that the stress relaxation causes deformation of the glass fibers even below the glass transition temperature. The stress decreases with time for a fixed strain as the deformation proceeds. Before the fiber is released from the cylinder at the time, t , the change of stress σ with time can be expressed using a single relaxation time system as follows.

$$\frac{d\sigma}{dt} = -\frac{\sigma}{\tau} \quad (7)$$

Eq. (7) is integrated to,

$$\sigma = \sigma_0 \exp\left(-\frac{t}{\tau}\right) \quad (8)$$

where σ_0 is the initial stress and τ is the relaxation time. The relaxation function $\Psi(t)$ is defined as follows

$$\Psi(t) = \frac{R_0}{R(t)} \quad (9)$$

The strain $\varepsilon(t)$ can then be written as a function of relaxation function $\Psi(t)$ as follows.

$$\varepsilon(r, t) = \Psi(t)\varepsilon_0(r) \quad (10)$$

where $\varepsilon_0(r) = r/R_0$, is the strain after infinite time. Using Eqs. (2), (3), (4), (8), and (10), Eq. (8) can be written as

$$1 - \Psi(t) = \exp\left(-\frac{t}{\tau}\right) \quad (11)$$

when the relaxation time spectrum is expressed as a distribution function, the relaxation mechanism can be analyzed by a non-linear relaxation function expressed by the Kohlrausch–Williams–Watts (KWW) equation, (stretched exponential decay function);

$$1 - \Psi(t) = \exp\left[\left(-\frac{t}{\tau}\right)^b\right] \quad 0 < b < 1 \quad (12)$$

where b is the stretching parameter, and ranges from 1 to 0. If the stretching parameter, b , is taken as 1, the KWW equation corresponds to Eq. (11). It is known that the relaxation time is distributed more diffusely as the stretching parameter b approaches zero.

3. Experimental Procedure

The chemical composition, Young's modulus, and glass transition temperature of the glass fibers used in this study are shown in Table 1. Differential thermal analysis

Table 1
The chemical composition, Young's modulus, and glass transition temperature of the glass fiber

Composition/mol%		Young's modulus/Pa	$T_g/^\circ\text{C}$ (10 K min^{-1})
SiO ₂	PbO		
50	50	4.41×10^{10} ^a	403

^a Ref. [18]

Table 2
The pre-annealing conditions and the heating conditions used for the bending method for determination of the viscosity of the glass fiber.

Glass no.	Pre-annealing		Annealing	
	Temp./ $^\circ\text{C}$	Time/min	Time/min	Temp./ $^\circ\text{C}$
1	–	–	200–240	0–2880
2	350	60	290–320	0–2880
3	350	600	320–350	0–2880
4	300	600	280–310	0–2880

(DTA) was used for determination of the glass transition temperature; the heating rate was 10 K min^{-1} . The diameters of the as-drawn and pre-annealed fibers were measured using an optical microscope. The glass fibers of about $100\ \mu\text{m}$ diameter were wound around cylinders of 3.0 cm radius. Quartz glass tubes were used as cylinders. Subsequently, these fibers were annealed at constant temperatures for various periods of time (Table 2). After annealing, the fibers were released and the bending radius of deformed fibers were measured by an image scanner connected to a computer.

4. Results

Figs. 3(a) and 3(b) show the profiles of the bending radius of the deformed fiber versus the annealing time at different temperatures below the glass transition temperature for glass numbers 1 and 2, respectively. The bending radius was obtained with an accuracy of $\pm 0.5\text{ mm}$. The temperature ranges of the measurement for glass numbers 1 and 2 are $200\text{--}250$ and $290\text{--}320^\circ\text{C}$, respectively. It was found that the bending radius decreases with increasing annealing temperature and time. This decrease is initially rapid, then slower, for longer annealing times for all glasses. For glass number 1, at temperatures above about 240°C the fiber takes nearly the same radius as that of cylinder. For glass number 2, below about 290°C no visible changes in the bending radius were seen especially for shorter annealing times.

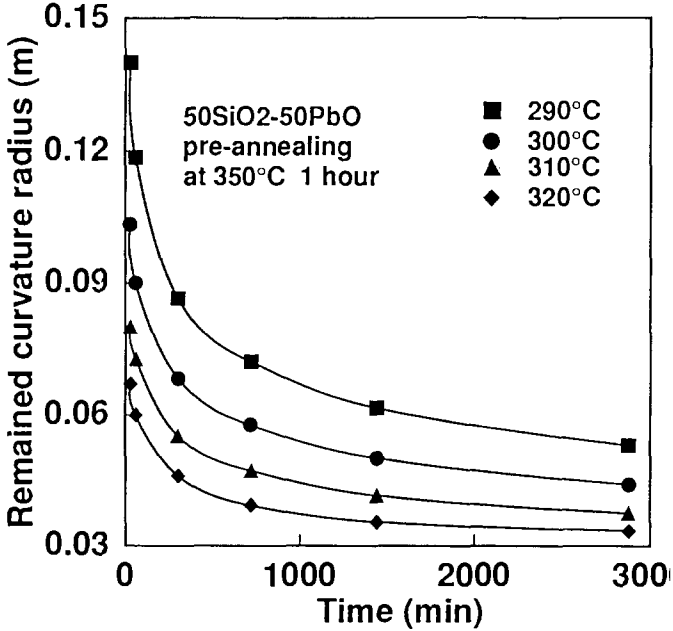
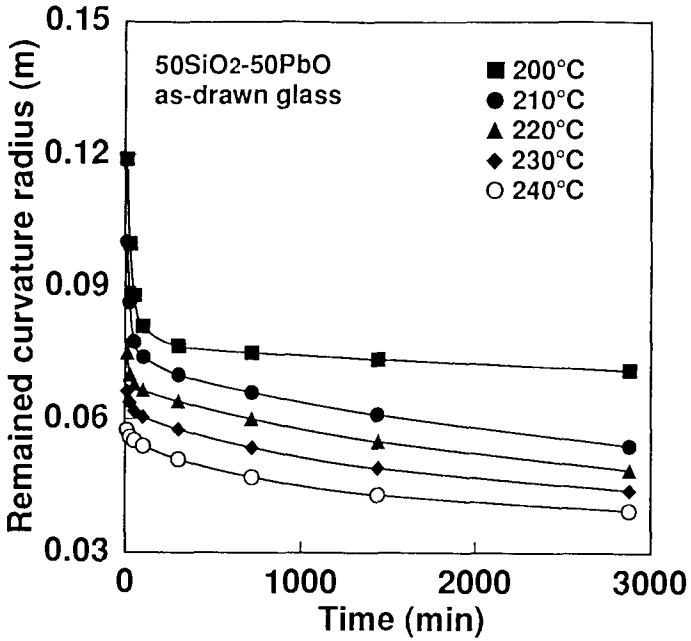


Fig. 3. The time-dependence of the residual curvature radius, $R(t)$, of (a) glass number 1 and (b) glass number 2.

Figs. 4(a) and 4(b) show the profiles of the residual strain at the outer surface versus the annealing time at different temperatures below the glass transition temperature for glass numbers 1 and 2, respectively. It is found that the residual strain increases with annealing time and temperature.

Figs. 5(a) and 5(b) show the profiles of the stress at the outer surface of the fiber versus the annealing time at different temperatures below the glass transition temperature for glass numbers 1 and 2, respectively. It is seen that the stress decreases with increasing annealing time and temperature.

5. Discussion

5.1. Changes of viscosity

As shown in Figs. 3(a) and 3(b), in all glasses it is clearly seen that the glass can deform at temperatures much lower than the glass transition temperature. The bending radius of the as-drawn glass fiber was measured at temperatures ranging from 200 to 240°C. However, the bending radius of the pre-annealed glass fiber at 350°C for 1 h was measured at higher temperatures (290 to 320°C) than those used for as-drawn glass. The sample preannealed at 350°C for 1 h is more stable than the as-drawn glass and requires a higher temperature for deformation.

Figs. 4(a) and 4(b) show the relationship between the residual strain at the outer surface and the annealing time for the as-drawn and the pre-annealed glass, respectively. The residual strains were determined from the plot of bending radius versus annealing time in Figs. 3(a) and 3(b) using Eq. (1). As the residual strain is inversely proportional to the bending radius, the profile of the curves in Fig. 4 will be the inverse of those in Fig. 3.

Figs. 5(a) and 5(b) show the relationship between the stress at the outer surface of the fiber, determined using Eqs. (3) and (4), and the annealing time for glass numbers 1 and 2, respectively. The stress decreases from the initial value with increasing annealing time. Plots of bending radius and residual strain and stress versus annealing time have similar features.

According to Eqs. (5) and (6), the viscosity can be calculated from the curves shown in Figs. 3–5. The viscosity of glass numbers 1 and 2 thus determined are shown as a function of the annealing time in Figs. 6(a) and 6(b), respectively. It is found that the viscosities of glass numbers 1 and 2 initially increase rapidly within a short annealing time and then continue to increase gradually, becoming nearly constant. The viscosity of the as-drawn glass fiber does not reach a equilibrium value over the working time for low annealing temperatures, e.g. 200 and 210°C. The change of the viscosity in the glass pre-annealed at 350°C for 1 h also continues to increase very slowly with time, even after 1500 min annealing.

The viscosities of 50:50 (mol%) PbO–SiO₂ glass have been measured above the glass transition temperature and near the liquidus using the penetration and the rotational methods, respectively [16,17]. Fig. 7 shows the variation of the viscosities with the reciprocal of temperature below and above the glass transition temperature. The viscosities below the glass transition temperature are those corresponding to the longer annealing time in Figs. 6(a) and 6(b). It is well known that above the glass

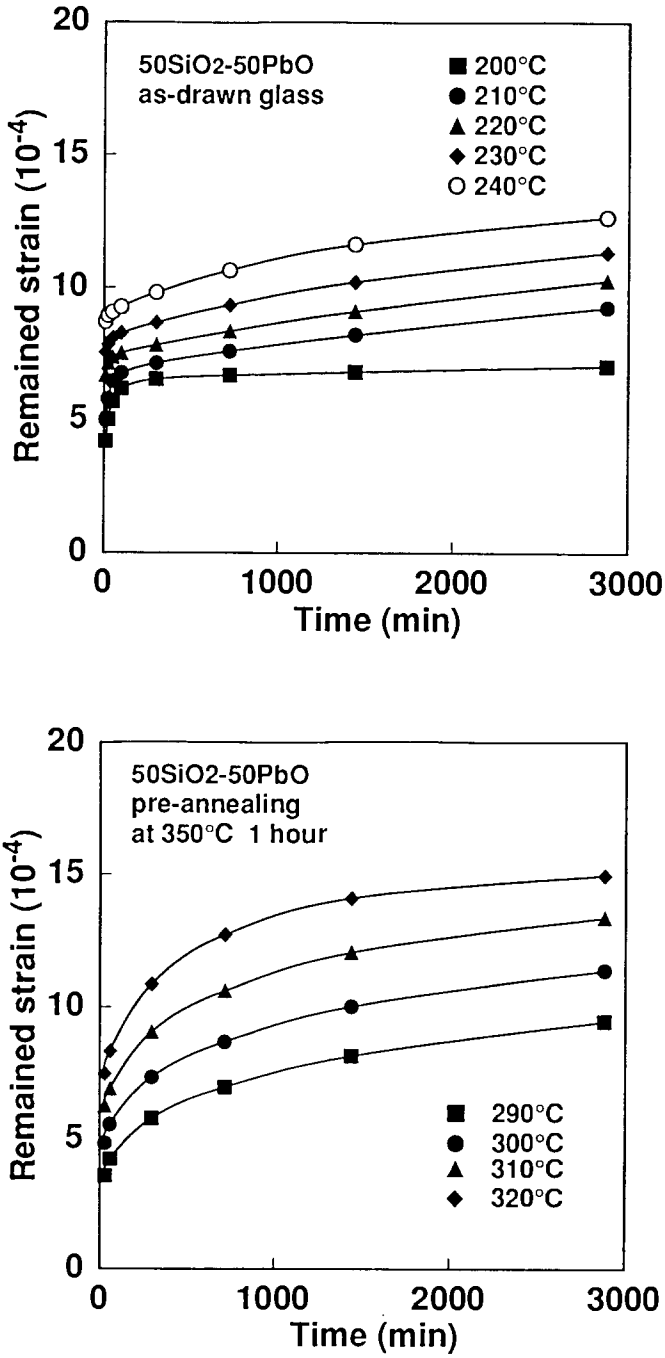


Fig. 4. The time-dependence of the residual strain, ϵ_{re} , at the outer surface of (a) glass number 1 and (b) glass number 2.

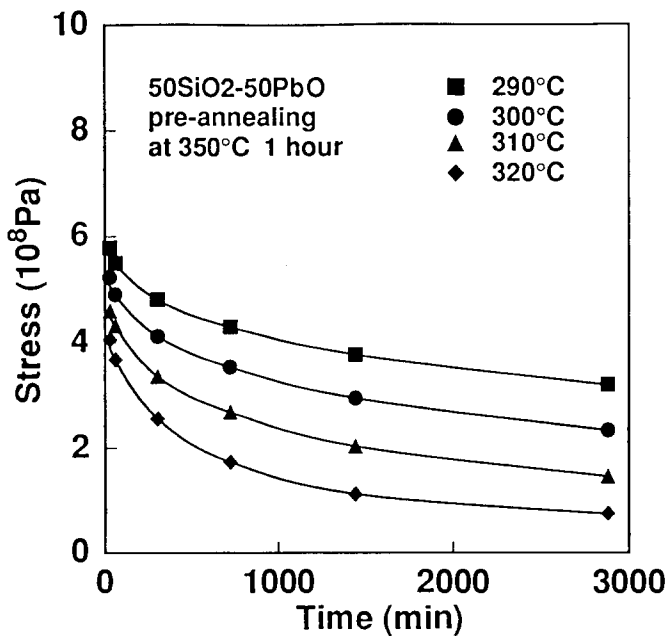
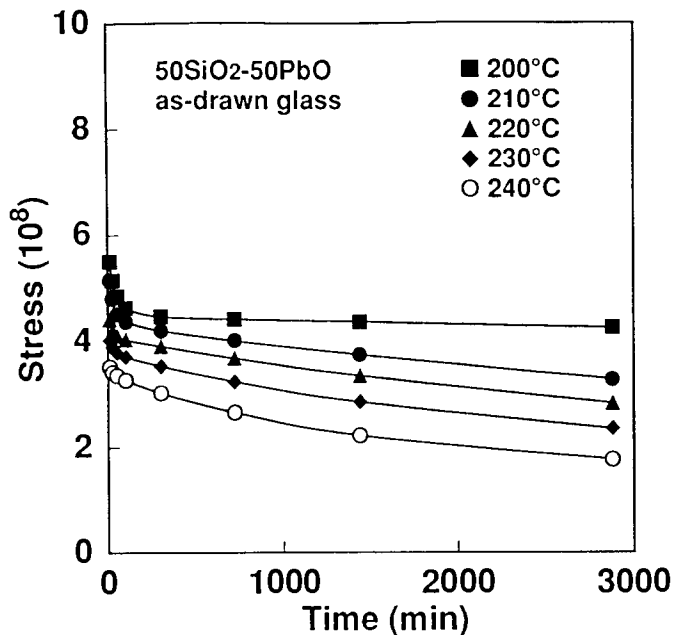


Fig. 5. The time-dependence of the stress, σ , at the outer surface of (a) glass number 1 and (b) glass number 2.

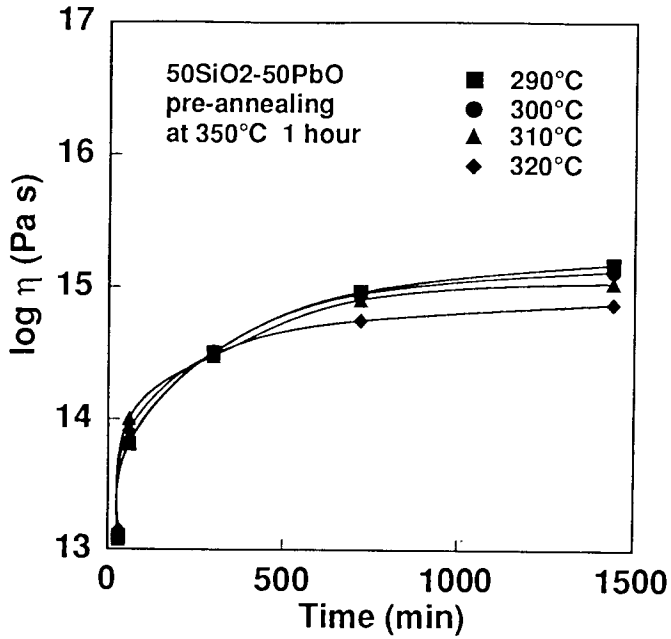
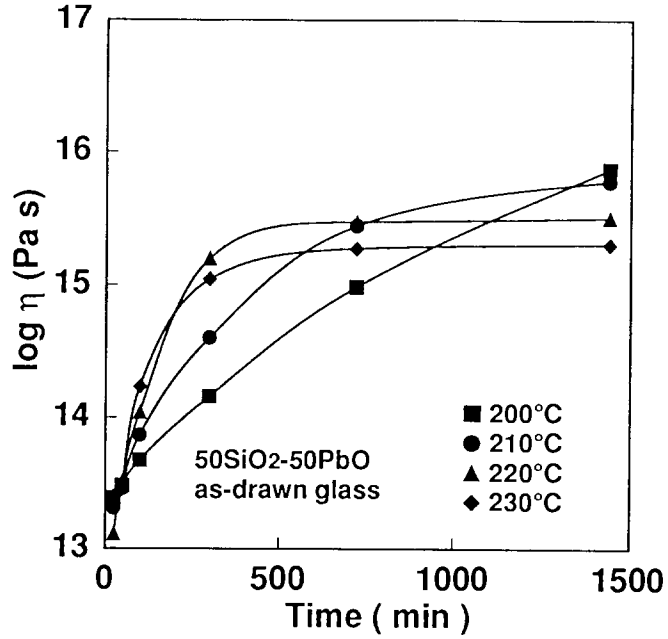


Fig. 6. The time-dependence of the viscosity of (a) glass number 1 and (b) glass number 2.

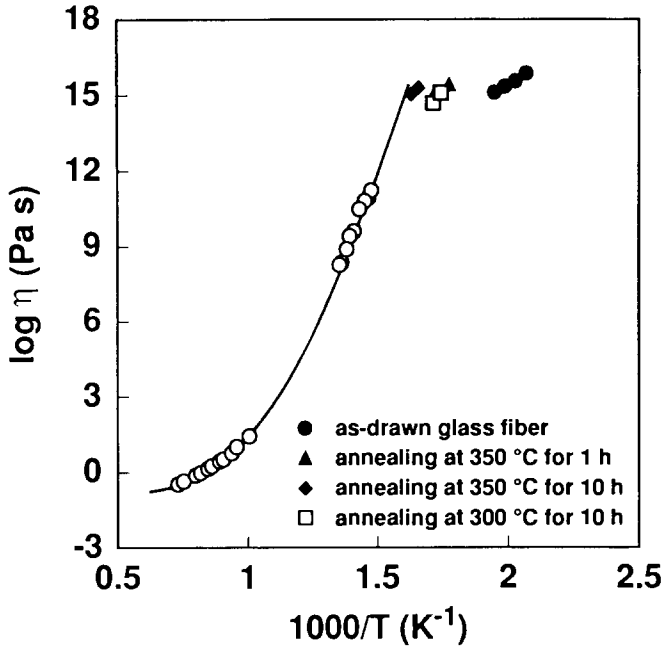


Fig. 7. The viscosity of glasses below and above the glass transition temperature.

transition temperature the viscosity obeys the Fulcher equation. However, it is seen that below the glass transition temperature the viscosity appears to obey the Arrhenius equation [11,14,19]. Taking this in account, it is clear that the viscosities increase with increasing pre-annealing temperature and time. The viscosity approaches the extrapolated line from the Fulcher equation above the glass transition temperature as the pre-annealing temperature and time increase. From this result it is suggested that the activation energy for viscous flow also increases with increasing pre-annealing temperature and time.

5.2. The relaxation mechanism

Stress relaxation mechanisms below the glass transition temperature were analyzed by means of a distribution function. The relaxation function, $\Psi = R_0/R(t)$, for glass numbers 1 and 2 is shown as a function of the logarithm of the annealing time in Figs. 8(a) and 8(b). Using these results, the time at which $\Psi = R_0/R(t) = 0.5$ was determined for each annealing temperature, and from these times the relaxation times, τ , can be determined. Eq. (12) can be written as

$$\log(-\ln(1 - \Psi)) = b \log\left(-\frac{t}{\tau}\right) \quad (13)$$

Figs. 9(a) and 9(b) show plots of $\log(-\ln(1 - \Psi))$ versus $\log(t/\tau)$ for glass numbers 1 and 2, respectively. The stretching parameter b were determined by least squares fit. The

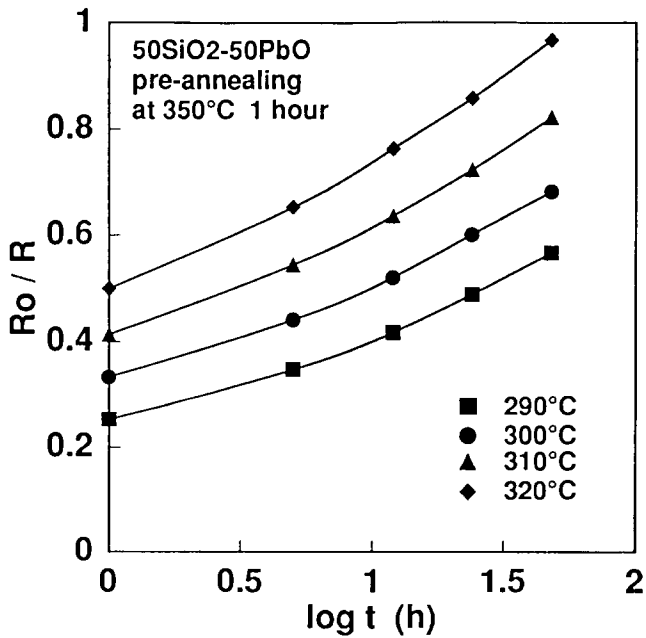
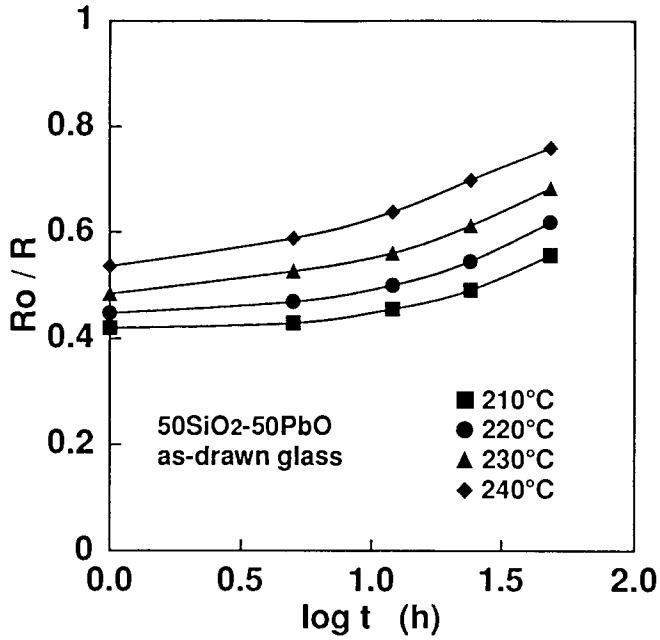


Fig. 8. The relaxation function after isothermal annealing of (a) glass number 1 and (b) glass number 2.

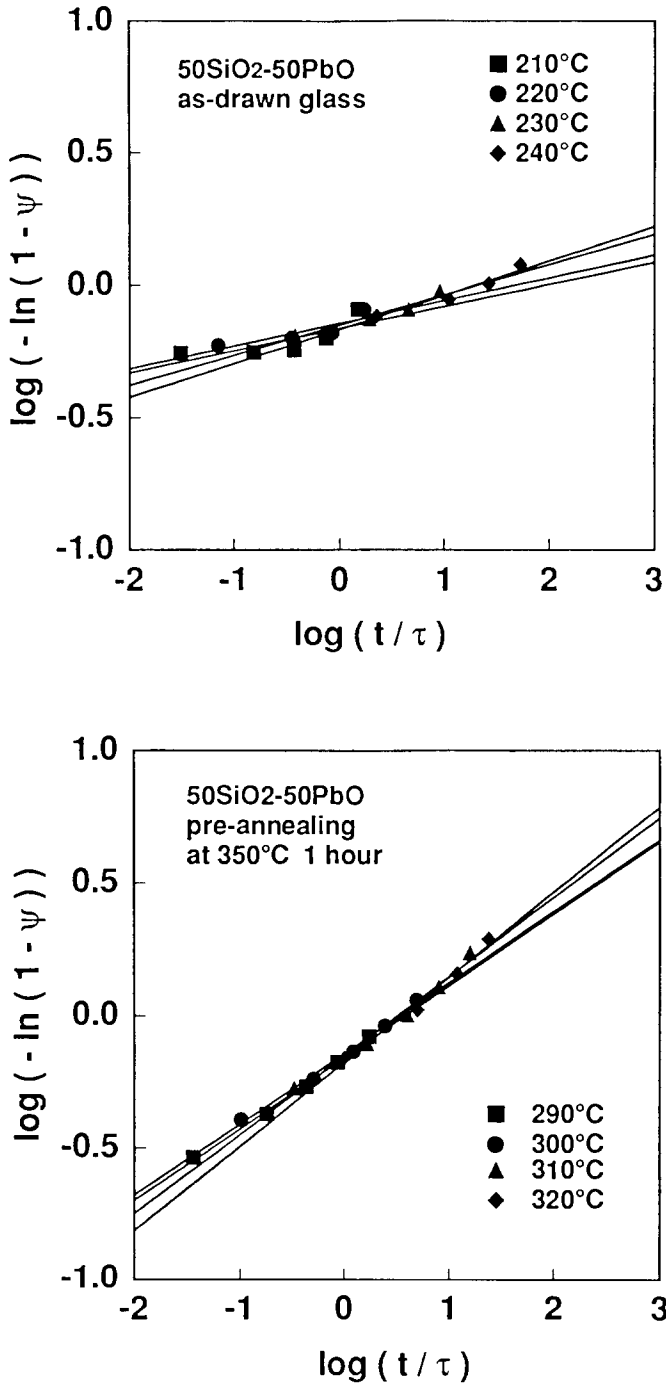


Fig. 9. Plot of $\log(t/\tau)$ versus $\log(-\ln(1-\Psi))$ for (a) glass number 1 and (b) glass number 2.

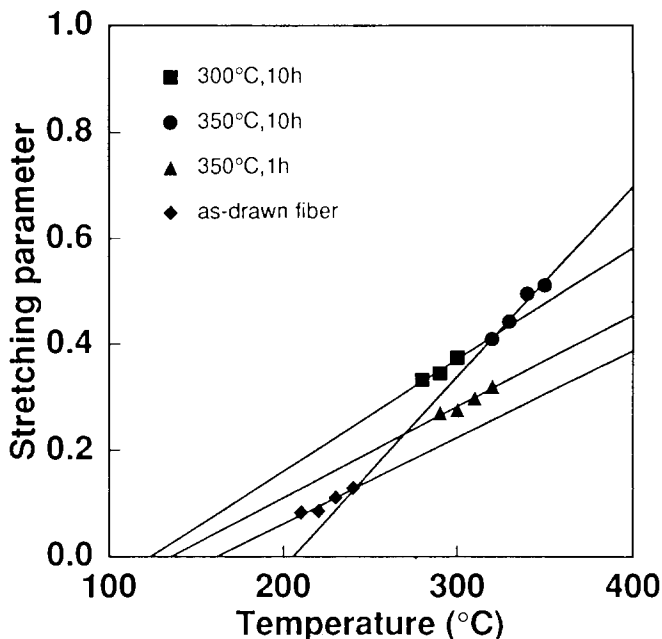


Fig. 10. The temperature-dependence of the stretching parameter.

stretching parameters, b , obtained are listed in Table 2 and Fig. 10 shows plots of annealing temperature versus the stretching parameter. The stretching parameter decreases with decreasing annealing temperature. This suggests wider distribution of relaxation time at lower temperatures and by extrapolation it was found that the stretching parameter is approximately 0.6 near the glass transition temperature. It is supposed that the as-drawn sample has many distortions and distributions of bond angles and bond length compared with the pre-annealed glass. Such distortions in glasses are reduced by pre-annealing even below the glass transition temperature, resulting in the higher stretching parameter.

6. Conclusion

The fiber-bending method was used for the measurement of the viscosity of glasses below the glass transition temperature. This method makes it possible to measure high viscosities in the range 10^{13} – 10^{16} Pa s. As-drawn and pre-annealed glass fibers under different conditions were used in the present study. It was found that the higher are pre-annealing temperature and the longer the pre-annealing time, the higher was the temperature required to wind the fiber on the cylinder. It was also found that the viscosity increases with increasing pre-annealing temperature and time. Furthermore, the viscosity approaches the extrapolated line from the Fulcher curve fitted for viscosity at temperatures above the glass transition temperature. By analyzing the

relaxation mechanism, it is found that the stretching parameter increases with increasing annealing temperature. This suggests wider distribution of the relaxation time at lower temperature; the stretching parameter is estimated, by extrapolation, to be approximately 0.6 near the glass transition temperature. This means that at the glass transition temperature the relaxation mechanism is composed of more than one mode.

Acknowledgements

This work was supported by the Nippon Sheet Glass Foundation for Materials Science. Part of this work is supported by the Power Reactor and Nuclear Fuel Development Corporation.

References

- [1] C.A. Angell, *J. Non-Cryst. Solids*, 73 (1985) 1.
- [2] K. Matusita, M. Koide and T. Komatsu, *J. Non-Cryst. Solids*, 140 (1992) 141.
- [3] A. Jha and J.M. Parker, *Phys. Chem. Glasses*, 30 (1989) 220.
- [4] E.H. Fontana and W.A. Plummer, *Phys. Chem. Glasses*, 7 (1965) 139.
- [5] C. Alba, L.E. Busse and C.A. Angell, *J. Chem. Phys.*, 92 (1990) 617.
- [6] M. Koide, K. Matusita and T. Komatsu, *J. Non-Cryst. Solids*, 125 (1990) 93.
- [7] K. Matusita, M. Koide and T. Komatsu, *J. Non-Cryst. Solids*, 140 (1992) 119.
- [8] K. Matusita, N. Osawa, M. Koide, R. Sato and T. Komatsu, *Proc. Japan–Russia–China Int. Seminar Struct. Formation Glasses*, The Ceramic Society of Japan, 217.
- [9] R. Sato, T. Komatsu and K. Matusita, *J. Non-Cryst. Solids*, 160 (1993) 180.
- [10] A.Q. Tool, *J. Am. Ceram. Soc.*, 29 (1946) 240.
- [11] W.H. Otto, *J. Am. Ceram. Soc.*, 44 (1961) 68.
- [12] O.V. Mazurin, Yu.K. Startsev and S.V. Stoljar, *J. Non-Cryst. Solids*, 52 (1982) 105.
- [13] J. De Bast and P. Gilard, *Phys. Chem. Glasses*, 4 (1963) 116.
- [14] M. Koide, R. Sato, T. Komatsu and K. Matusita, Viscosity of lead–silicate glasses below the glass transition temperature by the fiber-bending method, *Phys. Chem. Glasses*, 36(4) (1995) 172.
- [15] M. Koide, R. Sato, T. Komatsu and K. Matusita, Low temperature deformation of fluoride and oxide glass fibers below the glass transition temperature, *J. Non-Cryst. Solids*, 177 (1994) 427.
- [16] T. Ejima and M. Kameda, *J. Jpn Inst. Metals*, 31 (1967) 120. (In Japanese).
- [17] T. Kou, K. Mizoguchi and Y. Suginozawa, *J. Jpn Inst. Metals*, 42 (1978) 775 (in Japanese).
- [18] R.R. Shaw and D.R. Uhlmann, *J. Non-Cryst. Solids*, 5 (1971) 237.
- [19] A.L. Zijstra, *Phys. Chem. Glasses*, 4 (1963) 143.